Geoderma 241–242 (2015) 306–312

Contents lists available at ScienceDirect

Geoderma

journal homepage: www.elsevier.com/locate/geoderma

Inverse estimation of soil hydraulic properties under oil palm trees

Nor Suhada Abd Rashid [a], Muhamad Askari [b,*], Tadashi Tanaka [c], Jirka Simunek [d], Martinus Th. van Genuchten [e,f]

[a] Faculty of Civil Engineering, Univ. Teknologi Malaysia, 81310 Johor Bahru, Malaysia
[b] Institute of Environmental and Water Resources Management (IPASA), Univ. Teknologi Malaysia, 81310 Johor Bahru, Malaysia
[c] Dep. of International Affairs, Univ. of Tsukuba, Ibaraki 305-8577, Japan
[d] Dep. of Environmental Sciences, Univ. of California, Riverside, CA 92521, USA
[e] Dep. of Mechanical Engineering, Federal Univ. of Rio de Janeiro, UFRJ, Rio de Janeiro, RJ 21945-970, Brazil
[f] Dep. of Earth Sciences, Utrecht Univ., Budapestlaan 4, 3584CD Utrecht, Netherlands

ARTICLE INFO

Article history:
Received 17 August 2014
Received in revised form 29 November 2014
Accepted 4 December 2014
Available online 11 December 2014

Keywords:
Stemflow
Tension disc infiltrometer
Soil hydraulic properties
Oil palm
HYDRUS-2D/3D

ABSTRACT

Canopies of forested and agricultural ecosystems can significantly alter rainfall patterns into separate stemflow and throughfall areas. These two areas often have also different organic matter contents and soil compaction properties, and hence also soil hydraulic properties, thus causing further differences in the local infiltration rates close to and away from trees. In this study we analyzed possible differences in the unsaturated soil hydraulic properties of the stemflow and throughfall areas below an oil palm tree. Tension disc infiltrometer experiments were carried out underneath the canopy and in the interspace area of an oil palm tree plantation at successive tensions of 5, 2, and 0 cm. Soil hydraulic properties were estimated inversely from the measured data using the HYDRUS-2D/3D software package. Four van Genuchten soil hydraulic parameters (i.e., the residual water content, θ_r, the shape factors α and n, and the saturated hydraulic conductivity, K_s) were optimized. Saturated water contents, θ_s, were fixed at their laboratory-measured values. Initial estimates of the optimized parameters were set according to Wooding's solution, which ensured rapid convergence of the inverse solution. The stemflow and throughfall regions exhibited contrasting hydraulic properties as indicated by the estimated hydraulic parameters. Values of θ_s, α, n and K_s for the stemflow area were all found to be higher as compared to those of the throughfall area. The inverse solution using tension disc infiltrometer data proved to be very useful for rapid characterization of hydraulic properties of soil under the oil palm trees.

1. Introduction

This study focuses on possible differences in the physical and hydraulic properties of the stemflow and throughfall areas of oil palm trees. Previous studies have shown that stemflow can be a major source of tree-induced infiltration and subsequent flow in and below the soil root zone, including recharge (Aboal et al., 1999; Gomez et al., 2002; Liang et al., 2007, 2011; Pressland, 1976; Sansoulet et al., 2008; Tanaka et al., 1996). Liang et al. (2007) observed that cumulative stemflow per unit infiltration area along the downslope side of a tree trunk was nearly 20 times cumulative open-area rainfall. Sansoulet et al. (2008) similarly found that stemflow caused the infiltration rates around a banana stem to be up to six times higher than in the throughfall areas. Several other studies observed differences between stemflow and throughfall rates, including for olive trees (Gomez et al., 2002), banana plants (Cattan et al., 2009), tall stewartia (Liang et al., 2009), and ponderosa pine (Guan et al., 2010). While all of the above studies point to significant differences between the stemflow and throughfall rainfall rates, noticeably lacking are studies about possible differences in the soil hydraulic properties of the stemflow and throughfall areas, which should further exacerbate differences in the local infiltration rates.

The objective of the present study was to estimate the hydraulic properties characterizing the soil water retention and unsaturated hydraulic conductivity functions of soil underneath the stemflow and throughfall areas of an oil palm tree. Knowledge of these functions is essential to describe the movement of water and solutes in the vadose zone below the trees, including for ecohydrological studies and estimating local recharge rates.

A large number of direct and indirect approaches may be used to estimate the hydraulic properties of unsaturated soils. Neuman (1973) defined direct methods as those estimating the hydraulic conductivity and soil water retention directly from laboratory and/or field experiments. Numerous direct methods are available for this purpose as summarized well in several texts (Dane et al., 2002; Klute and Dirksen, 1986; van Genuchten et al., 1999). Unfortunately, direct methods have several limitations that restrict their use in practice in that they (i) are generally time consuming, especially for field-drainage experiments, (ii) are often difficult to implement for certain boundary conditions (especially for field conditions at relatively large scales), and (iii) often

* Corresponding author.
E-mail address: muhaskari@utm.my (M. Askari).

http://dx.doi.org/10.1016/j.geoderma.2014.12.003
0016-7061/

require steady-state flow conditions during the experiments. Information about uncertainty in the estimated hydraulic parameters is often also not readily derived using direct measurements. For these various reasons indirect approaches have become more popular recently.

Neuman (1973) defined indirect methods as parameter estimation methods involving the solution of an inverse problem. Inverse solutions based on the Richards equation are now increasingly used for estimating the unsaturated soil hydraulic properties. An advantage of this approach is that the retention and hydraulic conductivity functions can be estimated simultaneously from transient flow data, as shown by many past and recent studies (Abbasi et al., 2003; Abbaspour et al., 1999; Dane and Hruska, 1983; Eching and Hopmans, 1993; Kool and Parker, 1987; Lazarovitch et al., 2007; Minasny and Field, 2005; Ritter et al., 2003; Russo et al., 1991; Schwarzel et al., 2006; Sonnleitner et al., 2003; Zachmann et al., 1981). The soil hydraulic parameters are then obtained by minimizing an objective function, usually defined as the sum of squared deviations between observed and predicted transient water flow variables (Hopmans et al., 2002). In our study we used tension infiltration data for evaluating saturated and unsaturated hydraulic conductivities using the analytical approach of Wooding (1968). Tension disc infiltrometry has become a popular method for measuring in-situ cumulative infiltration functions and unsaturated hydraulic conductivities. The method has been used for many different soil types, climates, and vegetation covers (Ankeny et al., 1991; Kashkuli and Tangsir, 2011; Moret-Fernández et al., 2012; Schwartz et al., 2003; Schwen et al., 2011; Ventrella et al., 2005; Wahl et al., 2004). Examples of numerical studies in which tension infiltrometer data were used to inversely estimate the near-saturated soil hydraulic properties are by Simunek and van Genuchten (1997), Ramos et al. (2006) and Caldwell et al. (2013).

2. Material and methods

2.1. Field experiments

The field experiments were carried out at an oil palm plantation in Johor Darul Takzim, Malaysia. The plantation was established approximately 18 years ago. Based on the USDA soil classification scheme, surface soils at the plantation are sandy loams (about 77% sand, 10% silt, 13% clay). Soils in the area are typical oxisols (Selvaradjou et al., 2005) containing iron-rich parent materials such as serpentinite, basalt, andesite, schist and ferruginous shale. They are considered quite suitable for rubber and oil palm plantations.

Fig. 1 shows a layout of the palm trees in the measurement area, and the locations of the hydraulic measurements. The oil palm trees were planted using an equilateral triangular arrangement as shown in the figure. Measurements were carried out at four points within the throughfall area (TA) in the middle between trees, and at three points within the stemflow area (SA). Precise location of the SA points below the palm tree canopy was important to ensure overlap with the area where stemflow water infiltrated into the soil. Tanaka et al. (1991) found "litter marks" around the tree bases to be useful indicators of the infiltration area of stemflow-induced water. The infiltration area of stemflow-induced water, A_i, was estimated by the litter marks of oil palm trees. The area and equivalent radius of the litter marks from the center of the oil palm trunks were estimated by tape measurements. Previous studies (Tanaka, 2011; Tanaka et al., 1991, 1996) found that the extent of the litter marks at a given plantation is a function of the diameter of the tree base: the thicker the trunk, the more stemflow occurred and the more extensive the SA infiltration area. Iida et al. (2005) quantified this relationship for Formosa sweet gum and evergreen oak to obtain:

$$R_L = 23.36 \ln(D) - 31.53 \quad \left(R^2 = 0.753\right) \tag{1}$$

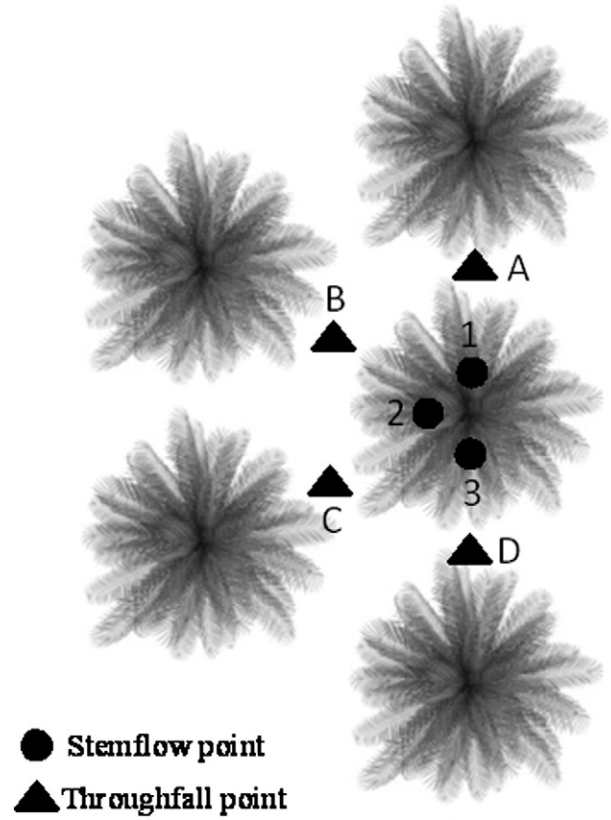

Fig. 1. Layout of the palm trees in the plantation and the measurement locations in the stemflow and throughfall areas.

where R_L is the radius (in cm) of the litter marks from the center of the stem, and D is the diameter of the tree base (in cm). We conducted several measurements to see if a similar relationship as Eq. (1) would hold also for our palm tree plantation.

A tension disc infiltrometer was used to conduct the field infiltration experiments in the stemflow (SA) and throughfall (TA) areas to obtain estimates of the soil hydraulic properties. Three successive tensions of 5, 2, and 0 cm were used for all infiltrometer experiments. The disc infiltrometer had a diameter of 20 cm and consisted of a nylon mesh. To ensure good contact between the disc and the soil, a thin (approximately 2 mm) layer of sand was placed on top of the soil. The sand layer was moistened just before placing the disc membrane on the soil in order to prevent air entry into the disc (Cameira et al., 2003).

Soil samples were collected additionally at depths of 0–10 cm at various measurement locations using a soil ring (height = 5 cm, diameter = 5 cm). In total 14 samples were collected to determine for each location the initial water content, θ_i, the bulk density, ρ_b, the organic matter content, OM, the total porosity, ε, and the residual water content, θ_r (the latter simply approximated initially by the wilting point).

2.2. Laboratory measurements

After performing the field experiments, laboratory measurements were carried out using the soil samples from the field. The initial water content was calculated by the loss of weight after oven-drying the samples at 105 °C for 24 h. Volumetric samples were used to determine the bulk density. The organic matter content was measured from loss-in-ignition (400 °C). Total porosity was estimated using the measured value of bulk density and a particle density of 2.65 g cm^{-3} (Post and Kwon, 2000; Rühlmann et al., 2006). Initial estimates of the residual water content were determined by measuring the water content at a pressure head of −15,000 cm using the pressure plate approach. Table 1 provides a summary of the laboratory measurements.

Table 1
Laboratory-measured data of the stemflow and throughfall areas of the oil palm plantation.

Location	Point	Initial water content θ_i ($cm^3\ cm^{-3}$)	Bulk density ρ_b ($g\ cm^{-3}$)	Total porosity ε (%)	Organic matter content OM (%)	Residual water content θ_r ($cm^3\ cm^{-3}$)
Stemflow area	1	0.350	1.173	55.7	0.492	0.291
	2	0.345	1.058	60.1	1.159	0.287
	3	0.341	1.275	51.9	0.290	0.288
Throughfall area	A	0.418	1.427	46.2	0.100	0.307
	B	0.447	1.366	48.4	0.134	0.349
	C	0.402	1.386	47.7	0.086	0.285
	D	0.376	1.327	49.9	0.087	0.288

2.3. Wooding's solution

The solution of Wooding (1968) has been used in many analyses of tension infiltration experiments. The solution assumes an exponential relationship for the hydraulic conductivity function applied to unconfined three-dimensional steady-state water infiltration (assuming zero ponding) from a circular source into the soil. The analysis is based on the following equations

$$Q(h_o) = \pi {r_o}^2 K(h_o) + 4r_o\phi(h_o) \tag{2}$$

$$\phi(h_o) = \int_{h_l}^{h_o} K(h)dh \tag{3}$$

$$K(h) = K_s \exp(\beta h) \tag{4}$$

where Q is the steady-state infiltration rate [$L^3\ T^{-1}$], r_o is the radius of the disc [L], K is the unsaturated hydraulic conductivity [$L\ T^{-1}$] derived from Gardner's model (Gardner, 1958), h_o is the supply wetting pressure head [L], h_l some fixed lower limit of the invoked pressure head range [L], often assumed to be $-\infty$, $\phi(h_o)$ is the matrix flux potential [$L^2\ T^{-1}$], K_s is the saturated hydraulic conductivity [$L\ T^{-1}$], and β is an empirical shape factor [L^{-1}]. The steady-state flow theory forming the basis of Eq. (2) and its applications have been discussed previously in many studies (Clothier and Smettem, 1990; Perroux and White, 1988; Quadri et al., 1994; Warrick, 1992).

Different approaches may be used to analyze steady-state tension disc infiltrometer data using Eq. (2). In our study we used the simplified approach followed by Ankeny et al. (1991) and Reynolds and Elrick (1991). Ankeny et al. (1991) assumed that $A = K(h) / \phi(h)$ is constant within an interval between h_i and h_{i+1}. They then calculated the unsaturated hydraulic conductivity, $K(h_i)$ and $K(h_{i+1})$, for the steady state fluxes, $Q(h_i)$ and $Q(h_{i+1})$, at two different pressure heads, h_i and h_{i+1}, as follows:

$$Q(h_i) = \left[\pi {r_0}^2 + \frac{4r_o}{A}\right] K(h_i) \tag{5}$$

$$Q(h_{i+1}) = \left[\pi {r_o}^2 + \frac{4r_o}{A}\right] K(h_{i+1}). \tag{6}$$

Reynolds and Elrick (1991) further assumed a piecewise exponential function to estimate the hydraulic conductivity in the middle of two successively applied tensions, $h_{i+1/2} = (h_i + h_{i+1}) / 2$, by rearranging Eq. (2) to become:

$$K\left(h_{i+1/2}\right) = \frac{Q_{i+1/2}}{\left[\pi {r_0}^2 + \frac{4r_0}{A_{i+1/2}}\right]}. \tag{7}$$

A geometric mean of the actual infiltration rates, Q_i and Q_{i+1}, was used to calculate the average infiltration rate, $Q_{i+1/2}$:

$$Q_{i+1/2} = \exp\left(\frac{\ln Q_i + \ln Q_{i+1}}{2}\right). \tag{8}$$

Parameter A in Eqs. (5) and (6) for the interval between two-consecutive tensions is given by

$$A = \frac{\ln\left(Q_i/Q_{i+1}\right)}{\left(h_i - h_{i+1}\right)}. \tag{9}$$

2.4. Inverse solution approach

The numerical inversion approach was based on solution of the Richards equation for two-dimensional axisymmetric isothermal flow in a variably-saturated isotropic rigid porous medium (Warrick, 1992):

$$\frac{\partial\theta}{\partial t} = \frac{1}{r}\frac{\partial}{\partial r}\left(rK\frac{\partial h}{\partial r}\right) + \frac{\partial}{\partial z}\left(K\frac{\partial h}{\partial z} + K\right) \tag{10}$$

where θ is the volumetric soil water content [$L^3\ L^{-3}$], h is the pressure head [L], K is the hydraulic conductivity [$L\ T^{-1}$], t is time [T], r is the radial coordinate [L], and z is the vertical coordinate, positive upward in our study [L].

The initial and boundary conditions under a disc infiltrometer having a radius r_o are given by (Simunek et al., 2000; Warrick, 1992):

$$\theta(z,r,t) = \theta_i \quad (t = 0) \tag{11a}$$

$$h(r,z,t) = h_0(t) \quad (0<r<r_0, z = 0) \tag{11b}$$

$$\frac{\partial h(r,z,t)}{\partial z} = -1 \quad (r>r_0, z = 0) \tag{11c}$$

$$h(r,z,t) = h_i \quad \left(r^2 + z^2 \to \infty\right). \tag{11d}$$

The soil hydraulic functions used in the inversion problem are described using the equations (van Genuchten, 1980):

$$S_e(h) = \frac{\theta(h) - \theta_r}{\theta_s - \theta_r} = \begin{cases} \left[1 + (\alpha h)^n\right]^{-m} & h<0 \\ 1 & h \geq 0 \end{cases} \tag{12}$$

$$K(S_e) = \begin{cases} K_s {S_e}^{0.5}\left[1 - \left(1 - {S_e}^{1/m}\right)^m\right]^2 & h<0 \\ K_s & h \geq 0 \end{cases} \tag{13}$$

where S_e is effective saturation [−], θ_s and θ_r are the saturated and residual water contents, respectively [$L^3\ L^{-3}$], K_s is the saturated hydraulic conductivity [$L\ T^{-1}$], and n [−] and α [L^{-1}] are shape parameters, and $m = 1 - 1 / n$. Eqs. (12) and (13) contain five unknown soil hydraulics hydraulic parameters: θ_s, θ_r, α, n and K_s, which potentially could all be estimated inversely from tension infiltrometer and related data using

the DISC (Simunek et al., 2000) or HYDRUS-2D/3D (Simunek et al., 2008) software packages.

Simunek and van Genuchten (1996) found that cumulative infiltration rates measured with a tension disc infiltrometer at only one particular tension did not provide enough information to estimate more than two soil hydraulic parameters. Additional information, such as the water content corresponding to the last measured tension under the disc infiltrometer, was needed. They subsequently found that a combination of multiple-tension cumulative infiltration data and measured values of the initial and final water contents yielded unique solutions of the inverse problem (Simunek and van Genuchten, 1997).

The objective function used in our study for the parameter optimization process consisted of cumulative infiltration data, the saturated soil water content (approximated by porosity) and the water content at $h = -15{,}000$ cm. Eching et al. (1994) in their study used, in addition to the cumulative drainage data, also water contents as input for the inversion in order to optimize the soil water retention and hydraulic conductivity curves. The initial condition was given by measured initial water contents of both the stemflow and throughfall areas.

3. Results and discussion

3.1. Experimental results

We first verified the expected stemflow infiltration area by correlating observed litter marks around various trees in the oil palm plantation with measured tree base diameters. Results are shown in Fig. 2. We fitted an equation similar to Eq. (1) to the data to obtain

$$R_L = 98.25 \ln(D) - 154.17 \quad \left(R^2 = 0.735\right) \qquad [14]$$

where, as before, R_L is the radius (in cm) of the litter marks from the center of the stem, and D is the diameter (in cm) of the tree base. Eq. (14) has a similar shape as Eq. (1) over the range of measured data, but with R_L values about 2.5 times larger. Differences in the coefficients of Eqs. (1) and (14) are to be expected for different vegetations having different canopy structures, and for different weather and soil conditions. Still, Eq. (14) showed that the selected SA measurement points (160 cm from the center of the tree trunk) were well within the expected stemflow infiltration area.

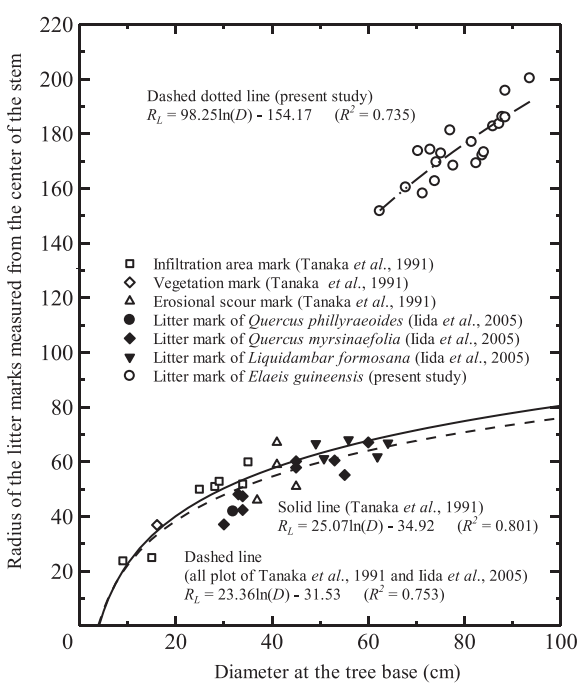

Fig. 2. Relationship between the diameter of the tree base (D, in cm) and the radius of the litter marks (R_L, in cm) measured from the center of the stem.

From the field tension disc infiltration data we obtained cumulative infiltration rates (Q) for all points under the stemflow (SA) and throughfall (TA) areas. Fig. 3 shows the measured infiltration rates obtained with three different supply pressure heads ($h = -5, -2$ and 0 cm). Notice the obvious breaks in the cumulative infiltration curves caused by adjusting the pressure heads at the new time intervals. Also, the slopes of the cumulative infiltration curves are different for the infiltration measurements at the three different supply pressure heads. Point 1 in the stemflow area required only approximately 70 min for 800 cm^3 of water to infiltrate, whereas Points 2 and 3 required 160 min for 600 cm^3 and 200 cm^3 of water to infiltrate, respectively. By comparison, the four points in the throughfall area showed similar infiltration patterns, with Points C and D requiring 160 min to infiltrate 400 cm^3 and 200 cm^3 of water into the soil. Except for SA Point 2, the cumulative infiltration curves indicate overall much higher infiltration rates for the stemflow area as compared to the throughfall area.

The laboratory measurements shown in Table 1 indicate that the stemflow area had a much higher porosity and higher organic matter content than the throughfall area. The organic matter contents were up to 13 times higher in the stemflow area. These results agree with measurements by Haron et al. (1998) who found that the avenues and weeded circles beneath oil palms had mean organic matter contents that increased with time after establishing the plantation: 0.82% after 5 years, 1.76% after 10 years and 2.21% after 20 years. A higher soil organic matter content is known to reduce the bulk density (Arvidsson, 1998) and soil compaction (Soane, 1990). Soil organic matter produced by trees is also known to improve the friability of otherwise tight soils, and to enhance soil structural development that will increase the infiltration capacity (Franzluebbers, 2002; Martin and Moody, 2001).

3.2. Hydraulic conductivities obtained using Wooding's solution

The infiltration rate data for both the stemflow and throughfall areas were used in the equations proposed by Ankeny et al. (1991) and Reynolds and Elrick (1991) as discussed earlier, to determine the unsaturated hydraulic conductivity. The approach of Ankeny et al. (1991) was used to calculate the unsaturated hydraulic conductivity from the steady state infiltration rates at two different tensions, while the approach of Reynolds and Elrick (1991) provided a piecewise exponential function for the hydraulic conductivity to yield estimates midway between two applied tensions. Fig. 4 shows a plot of the obtained hydraulic conductivity data versus pressure head. Although field measurements were carried out at only three pressure heads (-5, -2 and 0 cm), a relatively complete graph of the near-saturated hydraulic conductivity function, $K(h)$, could be obtained.

The results in Fig. 4 indicate that the saturated hydraulic conductivities (K_s) of the stemflow area were approximately six times higher as

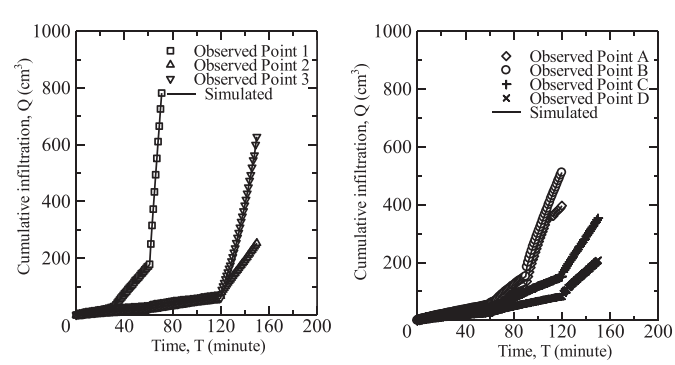

Fig. 3. Cumulative infiltration rates measured in the field and simulated using HYDRUS-2D/3D for the stemflow (left) and throughfall (right) areas.

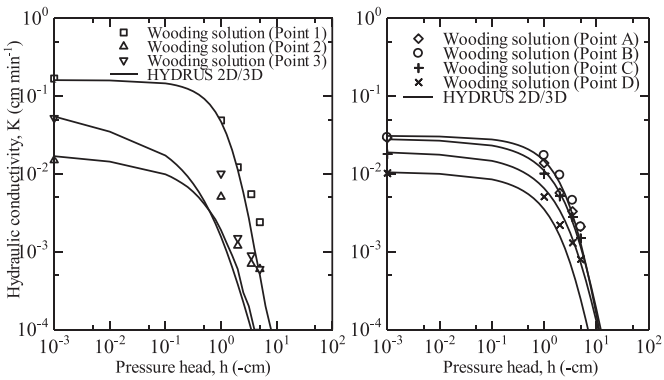

Fig. 4. Hydraulic conductivity data of the stemflow (left) and throughfall (right) areas as obtained using Wooding's solution and numerical inversion with HYDRUS-2D/3D.

those of the throughfall area. We next used the measured values of K_s of the stemflow and throughfall areas as initial values in the parameter estimation approach using HYDRUS-2D/3D.

3.3. Parameter estimation analysis

3.3.1. Optimized cumulative infiltration curves

Initial estimates of the saturated hydraulic conductivity were based on values obtained using Wooding's (1968) analysis. Tables 2a and 2b show the initial parameter values used in the parameter estimation analysis with HYDRUS. Of the various hydraulic parameters, saturated water contents (θ_s) were determined independently on soil samples in the laboratory and not optimized, while the initial values of the residual water content (θ_r) for each point in both areas were set equal to the laboratory-measured water contents at $h = -15{,}000$ cm.

Fig. 3 shows the measured and calculated cumulative infiltration curves when the objective function was defined in terms of the cumulative infiltration data. Results indicate excellent agreement between the measured and optimized infiltration curves. Results of the parameter optimization analyses with HYDRUS-2D/3D for both areas are listed in Tables 2a and 2b. The optimized parameter values for α, n and K_s were mostly very close or only slightly higher than the initial parameter values we used. The close correspondence of the initial and final estimates of K_s lends further credibility to the accuracy of Wooding's (1968) analysis of tension disc infiltrometer data, also for the tropical soils (oxisols) used in our study.

3.3.2. Hydraulic conductivity curves

Fig. 4 shows the near-saturated hydraulic conductivity curves for the stemflow and throughfall areas obtained with both Wooding's solution and the numerical inversion option of HYDRUS-2D/3D. Wooding's solution was found to give slightly higher values than the inverse solution, perhaps because steady-state infiltration conditions were not reached completely during the experiments, or the assumption of having an exponential hydraulic conductivity curve between each two pairs of infiltrometer data. Earlier work showed that Wooding's solution will overestimate the soil hydraulic conductivity if steady-state conditions are not achieved (Simunek et al., 1999). Also, tension infiltration experiments seldom reach complete saturation (Simunek and van Genuchten, 1996). The values of K_s for all points in the stemflow and throughfall areas as obtained with HYDRUS were essentially identical to the values derived using Wooding's solution. In all, relatively good agreement was obtained between the hydraulic conductivity functions derived with Wooding (1968) analysis and the numerical inversion using HYDRUS-2D/3D.

The measured soil physical properties (Table 1) indicate that the bulk density of the throughfall area was higher than that of the stemflow area, thus implying more compaction and a lower saturated conductivity. The higher bulk density is partly due to the much lower organic matter content of the throughfall area (see Table 1). Hudson (1994) found that soils having higher organic matter contents usually have a higher water holding capacity and a higher hydraulic conductivity, largely as a result of increased soil aggregation and the associated broader pore space distribution. But the higher bulk density of the throughfall area is in part also due to mechanical compaction by small pickup trucks used to collect oil palm branches and other material during harvesting. Antille et al. (2013) and Soane et al. (1980) showed that the use of agricultural machinery leads to higher bulk densities, and hence generally lower saturated hydraulic conductivities (Assouline, 2006; Dec et al., 2008), mostly because of a smaller volume of relatively coarse pores.

The higher near-saturated hydraulic conductivities of the stemflow area, along with the higher rates of stemflow reaching the soil surface, should combine to produce much higher infiltration rates as compared to the throughfall areas away from the palm trees.

3.3.3. Water retention curves

Fig. 5 shows the estimated soil water retention curves of the stemflow and throughfall areas as obtained with the numerical inversion approach using HYDRUS-2D/3D, including the laboratory-measured retention data at saturation and $h = -15{,}000$ cm. As expected, the data indicate higher saturated water contents for the stemflow area as compared to the throughfall area. Saturated water contents were up to 10% higher in the stemflow area. Since soil texture and soil type were relatively uniform across the oil palm plantation, differences in the water contents are due mostly to differences in the organic matter content (Table 1), and related differences in the bulk density, including those effects caused by wheel trafficking in the interspace area. Emerson (1995) found that higher soil organic matter contents strengthen soil aggregation, reduce soil compaction, and increase the water content. Rawls et al. (2003) similarly found that an increase in the organic matter content produced an increase in water retention of sandy soils. In addition, Wall and Heiskanen (2003) observed a significant positive correlation between the total porosity and the log-transformed organic matter content. However, a significant negative correlation was found between total porosity and bulk density.

The residual water content, θ_r, obtained with the inverse solution was close to the value of the water content at $h = -15{,}000$ cm measured in the laboratory. Because of the very coarse texture of the soil in our

Table 2a
Initial and optimized values of the soil hydraulic parameters of the stemflow area.

Hydraulic parameter	Initial value			Optimized value		
	Point 1	Point 2	Point 3	Point 1	Point 2	Point 3
θ_r (cm^3 cm^{-3})	0.291	0.287	0.288	0.291 ± 0.001	0.283 ± 0.02	0.279 ± 0.002
θ_s (cm^3 cm^{-3})	0.566	0.565	0.525	0.566[a]	0.565[a]	0.525[a]
α (cm^{-1})	0.329	0.196	0.327	0.508 ± 0.004	0.531 ± 0.012	0.908 ± 0.040
n (−)	1.543	1.378	1.337	2.032 ± 0.064	1.492 ± 0.027	1.340 ± 0.000
K_s (cm min^{-1})	0.1738	0.0157	0.0548	0.1605 ± 0.0034	0.0169 ± 0.0004	0.0549 ± 0.0000

[a] Not optimized.

Table 2b
Initial and optimized values of the soil hydraulic parameters of the throughfall area.

Hydraulic parameter	Initial value				Optimized value			
	Point A	Point B	Point C	Point D	Point A	Point B	Point C	Point D
θ_r (cm^3 cm^{-3})	0.307	0.349	0.285	0.288	0.306 ± 0.003	0.349 ± 0.001	0.283 ± 0.001	0.287 ± 0.001
θ_s (cm^3 cm^{-3})	0.485	0.534	0.496	0.490	0.485[a]	0.534[a]	0.496[a]	0.490[a]
α (cm^{-1})	0.156	0.191	0.167	0.145	0.214 ± 0.009	0.230 ± 0.003	0.210 ± 0.003	0.272 ± 0.002
n (−)	1.521	1.858	1.698	1.533	1.632 ± 0.098	1.794 ± 0.044	1.556 ± 0.023	1.642 ± 0.022
K_s (cm min^{-1})	0.0297	0.0297	0.0182	0.0105	0.0279 ± 0.0022	0.0308 ± 0.0010	0.0189 ± 0.0004	0.0105 ± 0.0003

[a] Not optimized.

study (77% sand), the water content at the permanent wilting point should be a very good estimate of the residual water content (van Genuchten, 1980). Including this value in the optimization was important since most or all of the data used in the optimization were in the wet range of the hydraulic properties. The water retention measurements at $h = -15{,}000$ cm hence served to fix the dry range of the hydraulic functions (Stephens and Rehfeldt, 1985). Contrary to expectations, the data indicated lower θ_r values for the stemflow area as compared to the throughfall area. According to Wall and Heiskanen (2003) and Saxton and Rawls (2006), the residual water content should increase with increasing organic matter content and the content of fine particles (especially clay particles). One possible reason may be the type of soil at our site. The θ_r values of our oxisol were higher as compared to class-average pedotransfer estimates obtained by Carsel and Parrish (1988) for temperate soils, but also higher than the average values obtained by Tomasella and Hodnett (1998) and Askari et al. (2008) for tropical soils in Brazil and Indonesia, respectively.

The optimized values of the α retention parameter (Tables 2a and 2b) for both areas were relatively large, indicative of the coarse nature of our soil (Carsel and Parrish, 1988; Fredlund and Xing, 1994). The value of α of the stemflow area was 2.8 times higher than that of throughfall area, which again reflects the lower bulk density and higher organic matter content of the stemflow area, leading to a more macroporous medium. By comparison, the values of n of the stemflow and throughfall areas were fairly similar, with the value of n for the stemflow area being slightly lower than for the throughfall area.

4. Conclusions

Our study showed that the saturated soil hydraulic conductivity (K_s) of the stemflow area around an oil palm tree was much higher (about 6 times) compared to the throughfall area. The saturated water content (θ_s) of the stemflow area was similarly higher about 10% higher than the saturated water content of the throughfall area. These results are significant in that they, if combined with the fact that stemflow rainfall rates are much higher than the throughfall rates, cause much higher local infiltration rates near the trees stem areas than in areas away from the trees, including open areas.

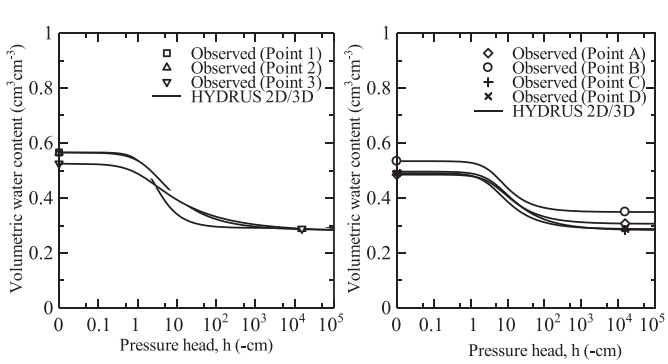

Fig. 5. Water retention curves for the stemflow (left) and throughfall (right) areas obtained using numerical inversion of the field-measured tension disc infiltrometer data.

Wooding's (1968) analytical solution, implemented here using a combination of the approaches of Ankeny et al. (1991) and Reynolds and Elrick (1991), proved to be very effective in estimating unsaturated hydraulic conductivities. Numerical inversion of the tension disc infiltrometer data provided a relatively simple, yet reliable alternative method for determining the water retention and hydraulic conductivity curves of near saturated soils. Including an independently measured water content (e.g., at −15,000 cm as done in our study) is important to better define the soil hydraulic functions in the dry range. We conclude that the HYDRUS inverse solution approach applied to infiltration data measured with a tension disc infiltrometer is a useful technique for rapid characterization of the unsaturated soil hydraulic properties.

Acknowledgment

The authors want to thank Dr. Rudiyanto from the Department of Civil and Environmental Engineering, Bogor Agricultural University, Indonesia, for his help with the numerical inversion methods using the HYDRUS-2D/3D software. This study was supported by the Ministry of Higher Education, Malaysia (vot number: R.J130000.7822.4F077) and Universiti Teknologi Malaysia Research University Grant (vot number: Q.J130000.2609.07J17), as well as by CAPES, Brazil.

References

Abbasi, F., Jacques, D., Simunek, J., Feyen, J., van Genuchten, M.T., 2003. Inverse estimation of soil hydraulic and solute transport parameters from transient field experiments: heterogeneous soil. Trans. ASAE 46 (4), 1097–1111.
Abbaspour, K., Sonnleitner, M., Schulin, R., 1999. Uncertainty in estimation of soil hydraulic parameters by inverse modeling: example lysimeter experiments. Soil Sci. Soc. Am. J. 63 (3), 501–509.
Aboal, J., Morales, D., Hernandez, M., Jimenez, M., 1999. The measurement and modelling of the variation of stemflow in a laurel forest in Tenerife, Canary Islands. J. Hydrol. 221 (3), 161–175.
Ankeny, M.D., Ahmed, M., Kaspar, T.C., Horton, R., 1991. Simple field method for determining unsaturated hydraulic conductivity. Soil Sci. Soc. Am. J. 55 (2), 467–470.
Antille, D.L., Ansorge, D., Dresser, M.L., Godwin, R.J., 2013. Soil displacement and soil bulk density changes as affected by tire size. Trans. ASABE 56 (5), 1683–1693.
Arvidsson, J., 1998. Influence of soil texture and organic matter content on bulk density, air content, compression index and crop yield in field and laboratory compression experiments. Soil Tillage Res. 49 (1–2), 159–170.
Askari, M., Tanaka, T., Setiawan, B.I., Saptomo, S.K., 2008. Infiltration characteristics of tropical soil based on water retention data. J. Jpn. Soc. Hydrol. Water Resour. 21, 215–227.
Assouline, S., 2006. Modeling the relationship between soil bulk density and the hydraulic conductivity function. Vadose Zone J. 5, 697–705.
Caldwell, T.G., Wohling, T., Young, M.H., Boyle, D.P., McDonald, E.V., 2013. Characterizing disturbed desert soils using multiobjective parameter optimization. Vadose Zone J. 12 (1).
Cameira, M., Fernando, R., Pereira, L., 2003. Soil macropore dynamics affected by tillage and irrigation for a silty loam alluvial soil in southern Portugal. Soil Tillage Res. 70 (2), 131–140.
Carsel, R.F., Parrish, R.S., 1988. Developing joint probability distributions of soil water retention characteristics. Water Resour. Res. 24 (5), 755–769.
Cattan, P., Ruy, S.M., Cabidoche, Y.M., Findeling, A., Desbois, P., Charlier, J.B., 2009. Effect on runoff of rainfall redistribution by the impluvium-shaped canopy of banana cultivated on an andosol with a high infiltration rate. J. Hydrol. 368 (1–4), 251–261.
Clothier, B., Smettem, K., 1990. Combining laboratory and field measurements to define the hydraulic properties of soil. Soil Sci. Soc. Am. J. 54 (2), 299–304.
Dane, J., Hruska, S., 1983. In-situ determination of soil hydraulic properties during drainage. Soil Sci. Soc. Am. J. 47 (4), 619–624.
Dane, J.H., Topp, C., Campbell, G.S., Horton, R., Jury, W.A., Nielsen, D.R., van Es, H.M., Wierenga, P.J., Topp, G.C., 2002. Part 4—Physical Methods. Methods of Soil Analysis.

Dec, D., Dörner, J., Becker-Fazekas, O., Horn, R., 2008. Effect of bulk density on hydraulic properties of homogenized and structured soils. J. Soil Sci. Plant Nutr. 8 (1), 1–13.
Eching, S., Hopmans, J., 1993. Optimization of hydraulic functions from transient outflow and soil water pressure data. Soil Sci. Soc. Am. J. 57 (5), 1167–1175.
Eching, S.O., Hopmans, J.W., Wendroth, O., 1994. Unsaturated hydraulic conductivity from transient multistep outflow and soil–water pressure data. Soil Sci. Soc. Am. J. 58 (3), 687–695.
Emerson, W., 1995. Water-retention, organic-C and soil texture. Soil Res. 33 (2), 241–251.
Franzluebbers, A.J., 2002. Water infiltration and soil structure related to organic matter and its stratification with depth. Soil Tillage Res. 66 (2), 197–205.
Fredlund, D.G., Xing, A., 1994. Equations for the soil–water characteristics curve. Can. Geotech. J. 31, 521–532.
Gardner, W., 1958. Some steady-state solutions of the unsaturated moisture flow equation with application to evaporation from a water table. Soil Sci. 85 (4), 228–232.
Gomez, J.A., Vanderlinden, K., Giraldez, J.V., Fereres, E., 2002. Rainfall concentration under olive trees. Agric. Water Manag. 55 (1), 53–70.
Guan, H., Simunek, J., Newman, B.D., Wilson, J.L., 2010. Modelling investigation of water partitioning at a semiarid ponderosa pine hillslope. Hydrol. Process. 24 (9), 1095–1105.
Haron, K., Brookes, P., Anderson, J., Zakaria, Z., 1998. Microbial biomass and soil organic matter dynamics in oil palm (*Elaeis guineensis* Jacq.) plantations, West Malaysia. Soil Biol. Biochem. 30 (5), 547–552.
Hopmans, J.W., Šimůnek, J., Romano, N., Durner, W., 2002. Inverse methods. In: Dane, J.H., Topp, G.C. (Eds.), Methods of Soil Analysis: Part 4 Physical Methods. Soil Science Society of America, Madison, WI, pp. 963–1008.
Hudson, B.D., 1994. Soil organic matter and available water capacity. J. Soil Water Conserv. 49 (2), 189–194.
Iida, S., Kakubari, J., Tanaka, T., 2005. "Litter marks" indication infiltration area of stemflow-induced water. Tsukuba Geoenviron. Sci. 1, 27–31.
Kashkuli, H.A., Tangsir, S., 2011. Comparison of two efficient methods for the estimation of field unsaturated hydraulic conductivity from disc permeameter measurements. World Appl. Sci. J. 14 (7), 1107–1114.
Klute, A., Dirksen, C., 1986. Conductivities and diffusivities of unsaturated soils. Methods Soil Anal. 1 687–734.
Kool, J., Parker, J., 1987. Development and evaluation of closed-form expressions for hysteretic soil hydraulic properties. Water Resour. Res. 23 (1), 105–114.
Lazarovitch, N., Ben-Gal, A., Simunek, J., Shani, U., 2007. Uniqueness of soil hydraulic parameters determined by a combined wooding inverse approach. Soil Sci. Soc. Am. J. 71 (3), 860–865.
Liang, W.L., Kosugi, K., Mizuyama, T., 2007. Heterogeneous soil water dynamics around a tree growing on a steep hillslope. Vadose Zone J. 6 (4), 879–889.
Liang, W.L., Kosugi, K., Mizuyama, T., 2009. Characteristics of stemflow for tall stewartia (*Stewartia monadelpha*) growing on a hillslope. J. Hydrol. 378 (1–2), 168–178.
Liang, W.L., Kosugi, K., Mizuyama, T., 2011. Soil water dynamics around a tree on a hillslope with or without rainwater supplied by stemflow. Water Resour. Res. 47 (2), 18.
Martin, D.A., Moody, J.A., 2001. Comparison of soil infiltration rates in burned and unburned mountainous watersheds. Hydrol. Process. 15 (15), 2893–2903.
Minasny, B., Field, D., 2005. Estimating soil hydraulic properties and their uncertainty: the use of stochastic simulation in the inverse modelling of the evaporation method. Geoderma 126 (3–4), 277–290.
Moret-Fernández, D., Latorre, B., González-Cebollada, C., 2012. Microflowmeter–tension disc infiltrometer: part II—hydraulic properties estimation from transient infiltration rate analysis. J. Hydrol. 466, 159–166.
Neuman, S.P., 1973. Calibration of distributed parameter groundwater flow models viewed as a multiple-objective decision process under uncertainty. Water Resour. Res. 9 (4), 1006–1021.
Perroux, K., White, I., 1988. Designs for disc permeameters. Soil Sci. Soc. Am. J. 52 (5), 1205–1215.
Post, W.M., Kwon, K.C., 2000. Soil carbon sequestration and land-use change: processes and potential. Glob. Chang. Biol. 6 (3), 317–327.
Pressland, A., 1976. Soil moisture redistribution as affected by throughfall and stemflow in an arid zone shrub community. Aust. J. Bot. 24 (5), 641–649.
Quadri, M., Angulo-Jaramillo, R., Vauclin, M., Clothier, B., Green, S., 1994. Axisymmetric transport of water and solute underneath a disk permeameter: experiments and numerical model. Soil Sci. Soc. Am. J. 58 (3), 696–703.
Ramos, T., Gonçalves, M., Martins, J., van Genuchten, M.T., Pires, F., 2006. Estimation of soil hydraulic properties from numerical inversion of tension disk infiltrometer data. Vadose Zone J. 5 (2), 684–696.
Rawls, W.J., Pachepsky, Y.A., Ritchie, J.C., Sobecki, T.M., Bloodworth, H., 2003. Effect of soil organic carbon on soil water retention. Geoderma 116 (1–2), 61–76.
Reynolds, W., Elrick, D., 1991. Determination of hydraulic conductivity using a tension infiltrometer. Soil Sci. Soc. Am. J. 55 (3), 633–639.
Ritter, A., Hupet, F., Munoz-Carpena, R., Lambot, S., Vanclooster, M., 2003. Using inverse methods for estimating soil hydraulic properties from field data as an alternative to direct methods. Agric. Water Manag. 59 (2), 77–96.
Rühlmann, J., Körschens, M., Graefe, J., 2006. A new approach to calculate the particle density of soils considering properties of the soil organic matter and the mineral matrix. Geoderma 130 (3–4), 272–283.
Russo, D., Bresler, E., Shani, U., Parker, J.C., 1991. Analyses of infiltration events in relation to determining soil hydraulic properties by inverse problem methodology. Water Resour. Res. 27 (6), 1361–1373.
Sansoulet, J., Cabidoche, Y.-M., Cattan, P., Ruy, S., Šimůnek, J., 2008. Spatially distributed water fluxes in an andisol under banana plants: experiments and three-dimensional modeling. Vadose Zone J. 7 (2), 819–829.
Saxton, K.E., Rawls, W.J., 2006. Soil water characteristic estimates by texture and organic matter for hydrologic solutions. Soil Sci. Soc. Am. J. 70 (5), 1569–1578.
Schwartz, R.C., Evett, S.R., Unger, P.W., 2003. Soil hydraulic properties of cropland compared with reestablished and native grassland. Geoderma 116 (1), 47–60.
Schwarzel, K., Simunek, J., Stoffregen, H., Wessolek, G., van Genuchten, M.T., 2006. Estimation of the unsaturated hydraulic conductivity of peat soils. Vadose Zone J. 5 (2), 628–640.
Schwen, A., Bodner, G., Scholl, P., Buchan, G., Loiskandl, W., 2011. Temporal dynamics of soil hydraulic properties and the water-conducting porosity under different tillage. Soil Tillage Res. 113 (2), 89–98.
Selvaradjou, S.K., Montanarella, L., Spaargaren, O., Dent, D., Filippi, N., Dominik, S., 2005. Metadata of the Soil Maps of Asia. Office of the Official Publications of the European Communities, Luxembourg.
Simunek, J., van Genuchten, M.T., 1996. Estimating unsaturated soil hydraulic properties from tension disc infiltrometer data by numerical inversion. Water Resour. Res. 32 (9), 2683–2696.
Simunek, J., van Genuchten, M.T., 1997. Estimating unsaturated soil hydraulic properties from multiple tension disc infiltrometer data. Soil Sci. 162 (6), 383–398.
Simunek, J., Wendroth, O., van Genuchten, M., 1999. Estimating unsaturated soil hydraulic properties from laboratory tension disc infiltrometer experiments. Water Resour. Res. 35 (10), 2965–2979.
Simunek, J., van Genuchten, M.T., Sejna, M., 2000. The DISC computer software for analyzing tension disc infiltrometer data by parameter estimation. Version 1.0. U.S. Salinity Laboratory, Riverside, California.
Simunek, J., van Genuchten, M.T., Sejna, M., 2008. Development and applications of the HYDRUS and STANMOD software packages and related codes. Vadose Zone J. 7 (2), 587–600.
Soane, B.D., 1990. The role of organic matter in soil compactibility: a review of some practical aspects. Soil Tillage Res. 16 (1–2), 179–201.
Soane, B.D., Blackwell, P.S., Dickson, J.W., Painter, D.J., 1980. Compaction by agricultural vehicles: a review II. Compaction under tyres and other running gear. Soil Tillage Res. 1, 373–400.
Sonnleitner, M., Abbaspour, K., Schulin, R., 2003. Hydraulic and transport properties of the plant–soil system estimated by inverse modelling. Eur. J. Soil Sci. 54 (1), 127–138.
Stephens, D.B., Rehfeldt, K.R., 1985. Evaluation of closed-form analytical models to calculate conductivity in a fine sand1. Soil Sci. Soc. Am. J. 49 (1), 12–19.
Tanaka, T., 2011. Effects of the canopy hydrologic flux on groundwater. In: Levia, D.F., Carlyle-Moses, D., Tanaka, T. (Eds.), Forest Hydrology and Biogeochemistry: Synthesis of Past Research and Future Directions. Springer, pp. 499–518.
Tanaka, T., Tsujimura, M., Taniguchi, M., 1991. Infiltration area of stemflow-induced water. Annual Report-Institute of Geoscience 17. University of Tsukuba, pp. 30–32.
Tanaka, T., Taniguchi, M., Tsujimura, M., 1996. Significance of stemflow in groundwater recharge. 2. A cylindrical infiltration model for evaluating the stemflow contribution to groundwater recharge. Hydrol. Process. 10 (1), 81–88.
Tomasella, J., Hodnett, M.G., 1998. Estimating soil water retention characteristics from limited data in Brazilian Amazonia. Soil Sci. 163 (3), 190–202.
van Genuchten, M.T., 1980. A closed-form equation for predicting the hydraulic conductivity of unsaturated soils. Soil Sci. Soc. Am. J. 44 (5), 892–898.
van Genuchten, M.T., Schaap, M., Mohanty, B., Simunek, J., Leij, F., 1999. Modeling Flow and Transport Processes at the Local Scale. Modelling of Transport Process in Soils at Various Scales in Time and Space. Wageningen Pers, Wageningen, the Netherlands, pp. 23–45.
Ventrella, D., Losavio, N., Vonella, A., Leij, F., 2005. Estimating hydraulic conductivity of a fine-textured soil using tension infiltrometry. Geoderma 124 (3–4), 267–277.
Wahl, N.A., Bens, O., Buczko, U., Hangen, E., Hüttl, R., 2004. Effects of conventional and conservation tillage on soil hydraulic properties of a silty-loamy soil. Phys. Chem. Earth A/B/C 29 (11), 821–829.
Wall, A., Heiskanen, J., 2003. Water-retention characteristics and related physical properties of soil on afforested agricultural land in Finland. For. Ecol. Manag. 186 (1–3), 21–32.
Warrick, A.W., 1992. Models for disk infiltrometers. Water Resour. Res. 28 (5), 1319–1327.
Wooding, R., 1968. Steady infiltration from a shallow circular pond. Water Resour. Res. 4 (6), 1259–1273.
Zachmann, D.W., Duchateau, P.C., Klute, A., 1981. The calibration of the Richards flow equation for a draining column by parameter identification. Soil Sci. Soc. Am. J. 45, 1012–1015.